Remagnetization Strategies for Induction Machines Operating with Reduced Flux Levels

Ahmed F. Abouzeid, *Student Member, IEEE* , Juan M. Guerrero, *Senior Member, IEEE*, Iban Vicente, Iker Muniategui, Aitor Endemaño, and Fernando Briz, *Senior Member, IEEE*

***Abstract*—Induction Machines (IMs) drives are the preferred option for high-speed railway traction drives. Electric drives in this application can work for certain periods of time with light load levels. It is possible in this case to decrease the flux level to reduce the stator current and consequently both joule and hysteresis losses. A drawback of this approach is that if a torque increase is demanded, the machine must be firstly remagnetized. Remagnetization time is determined by the rotor time constant and the applied magnetizing current. Due to the relatively large values of the rotor time constant, fast torque changes are not feasible, which eventually penalizes the dynamic response of the drive. This paper presents strategies for the remagnetization of Induction Machines. Though proposed methods are primarily intended for railways traction, they can be easily extended to other uses of IM drives.**

***Index Terms*—Induction Machines; Field-Oriented Control; Scalar Control; Maximum-Torque-Per-Ampere (MTPA); Remagnetization.**

I. INTRODUCTION

TRACTION electrification gained more attention in recent years due to fuel costs and environmental concerns. Thanks to the continuous development of renewable energy conversion systems and power electronic converters, the electric traction drive systems (ETDS) have been drastically improved [1]. Efficiency, performance, torque and power densities are the key aspects of ETDSs. Compromising these aspects over a wide speed range is a challenging task. This can be achieved either by traction machine type, electric drive control, or a combination of both [2]. Permanent-magnet (PM) synchronous machines are widely used for traction applications due to their high efficiency, high torque, and high power densities [3]. However, cost and rare-earth material availability are the main limitations of PMs [4]. Induction machines (IMs), besides being robust with fewer maintenance requirements, are considered the promising alternative of PMs in traction applications [5]. Rewinding the machine combined with optimized control techniques of the electric drive, IMs can achieve comparable performance to PMs [6], [7]. Furthermore, for specific applications like traction, the overall efficiency of the IM operating at partial load can be improved by reducing the air gap flux level [8].

IMs control optimization techniques objective may include minimization of total losses, maximization of power transfer and/or maximization of torque production [9], [10]. Optimal efficiency control or also called loss minimization control aims to select the appropriate machines' flux level minimizing the joule and hysteresis losses of the machine [11]. Maximum-Torque-per-Ampere (MTPA) method aims to optimally select the flux and torque producing components of machines' stator current to achieve maximum torque with minimum losses considering inverter voltage limits [12]. Similarly, Maximum-Torque-per-Voltage (MTPV) method is used to fulfill the optimization criteria taking into consideration both inverter voltage and current constraints [10].

Regardless of the optimization technique used, the IM operates at a reduced flux level during light loads. Hence, at any instant, if the load torque is increased, the machine flux has to be re-established (i.e. remagnetized) quickly for producing the required torque. While the aforementioned optimization techniques are intended for steady-state operation, an additional approach should be imposed to control the transient dynamics. Few attempts have been made for improving the transient response and minimizing the machine's losses during flux remagnetization. In [13], an optimal dynamic current sharing algorithm is proposed to mitigate machine speed drops for sudden torque increases while the machine is initially operating at reduced flux. Alternative power loss minimization techniques using model predictive control in transient states of speed controller machines are presented in [14], [15]. In [16], different stator current sharing techniques have been proposed for improving the dynamic response of the IM, however, the proposed methods were intended for Field Oriented Control (FOC) schemes.

In this paper, the problem of operating the IM with reduced flux will be addressed. In addition, different flux remagnetization strategies considering the dynamic response and inverter limits will be proposed. The proposed strategy generates the optimum torque and flux trajectories that meet the application requirements and it can be used for vector and scalar control schemes.

Ahmed Fathy Abouzeid is with the Department of Electrical, Electronic and Computer Engineering, University of Oviedo, Gijón, Spain (e-mail: abouzeidahmed@uniovi.es). He is on leave with the Department of Electrical Engineering, Port-Said University, Egypt (e-mail: ahmed_abouzeid@eng.psu.edu.eg).

Iban Vicente, Iker Muniategui, Aitor Endemaño are with the Department of Traction systems, Ingeteam Power Technology, Zamudio, Spain (e-mail: iban.vicente@ingeteam.com; iker.muniategui@ingeteam.com; aitor.endemano@ingeteam.com).

Juan Manuel Guerrero and Fernando Briz are with the Department of Electrical, Electronic and Computer Engineering, University of Oviedo, Gijón, Spain (e-mail: guerrero@uniovi.es; fbriz@uniovi.es).

This work was supported in part by Government of Asturias under project AYUD/2021/50988.

II. Modelling, operating regions and control of induction machines

A. IM model using complex vector notation

Complex vectors are a powerful tool for the modeling of three-phase symmetric ac machines [17]. The sinusoidal variation of mutual inductances with respect to the rotor angle is eliminated by transforming the electrical variables of stator and rotor to a common reference frame. This frame can be either fixed to the stator or rotated with the electromagnetic quantities of the machine, being denoted as stationary and synchronous reference frames respectively [18]. In this paper, rotor-flux field-orientation (RFOC) will be used as it allows decoupled control of rotor flux and torque [19].

Stator voltage equation in a rotor-flux reference frame is given by (1), where σL_s is the stator transient inductance, R_s' is stator transient resistance and τ_r is the rotor time constant (2); R_s and R_r are the stator and rotor resistances, respectively; L_s, L_r, and L_m are the stator, rotor, and mutual inductances, respectively; ω_e is the rotor flux angular frequency; ω_r is the rotor angular frequency.

Rotor flux and torque equations for the IM in the rotor-flux reference frame are given by (3)-(4), with P being the number of pole-pairs. The slip frequency ω_{slip} is given by (5), the rotor flux angular frequency ω_e and angle θ_e being obtained as shown in (6).

$$v_{dqs} = \sigma L_s \frac{di_{dqs}}{dt} + (R_s' + \sigma L_s j\omega_e)\, i_{dqs} - \frac{L_m}{L_r}\left(\frac{1}{\tau_r} - j\omega_r\right)\lambda_r \tag{1}$$

$$\sigma = 1 - \frac{L_m^2}{L_s L_r};\ \ R_s' = R_s + \left(\frac{L_m}{L_r}\right)^2 R_r;\ \ \tau_r = \frac{L_r}{R_r} \tag{2}$$

$$\frac{d\lambda_r}{dt}\tau_r + \lambda_r = L_m i_{ds} \tag{3}$$

$$T_e = \frac{3}{2} P \frac{L_m}{L_r} \lambda_{dr} i_{qs} \tag{4}$$

$$\omega_{slip} = \frac{L_m}{\tau_r \lambda_r} i_{qs} \tag{5}$$

$$\omega_e = \omega_r + \omega_{slip};\quad \theta_e = \int \omega_e dt \tag{6}$$

B. Regions of operation of the IM

Fig. 1 shows the operating regions of IMs considering that torque reduction and field weakening occur at the same frequency at which the inverter reaches its voltage limit. The full range of operation is considered: 1) MTPA; 2) rated flux; 3) field weakening region I, and 4) field weakening region II. Transitions from region 2) to 3) and from region 3) to 4) are the result of voltage constraints. In segment 4-5 the machine operates with MTPV operation. The behavior and constraints of the machine in steady-state are defined by the stator voltage equation (7) (determined by dc-link voltage V_{dc} and modulation strategy, being $v_{dqs_{limit}} = V_{dc}/\sqrt{3}$ for linear operation of inverter), current limit (mainly due to thermal issues) (8) where V_{dc} is the dc-link voltage.

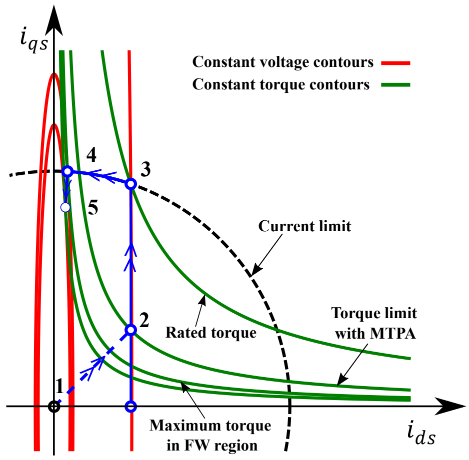

Fig. 1: Regions of operation of the induction machine for the case rated voltage and rated speed occur at the same frequency (Segment 1-2: MTPA region; Segment 2-3: rated flux region; Segment 3-4: field weakening region 1; Segment 4-5: field weakening region 2 (MTPV)).

$$(\omega_e \sigma L_s i_{qs})^2 + (\omega_e L_s i_{ds})^2 \leq v_{dqs_{limit}}^2 \tag{7}$$

$$\sqrt{i_{ds}^2 + i_{qs}^2} \leq i_{dqs_{rated}} \tag{8}$$

MTPA can be implemented in segment 1-2 (see Fig. 1) while operation at rated flux applies between 2 and 3. In point 3 the machine operates at is rated values of voltage (9), current (10).

$$(\omega_e \sigma L_s i_{qs_{rated}})^2 + (\omega_e L_s i_{ds_{rated}})^2 = v_{dqs_{limit}}^2 \tag{9}$$

$$i_{qs_{rated}} = \sqrt{i_{dqs_{rated}}^2 - i_{ds_{rated}}^2};\ i_{ds_{rated}} = \frac{\lambda_{r_{rated}}}{L_m} \tag{10}$$

Field weakening region I corresponds to the segment 3-4 in Fig. 1. In this region, the machine operates with rated voltage and current, but with reduced d-axis current and therefore reduced rotor flux. The d-axis current can be written as a function of the fundamental frequency (11), which is obtained from (8) and (9), the q-axis current being (12). The maximum fundamental frequency in field weakening region I occurs when the constant voltage ellipsis and the constant torque hyperbola do not intersect to each other but the ellipsis become tangent (operating point 4 in Fig. 1).

$$i_{ds} = \sqrt{\frac{\left(\frac{v_{dqs_{limit}}}{\omega_e}\right)^2 - (\sigma L_s i_{dqs_{rated}})^2}{L_s^2\,(1-\sigma^2)}} < i_{ds_{rated}} \tag{11}$$

$$i_{qs} = \sqrt{i_{dqs_{rated}}^2 - i_{ds}^2} = \sqrt{\frac{\left(L_s i_{dqs_{rated}}\right)^2 - \left(\frac{v_{dqs_{limit}}}{\omega_e}\right)^2}{L_s^2\left(1-\sigma^2\right)}} \tag{12}$$

In field weakening region II (see segment 4-5 in Fig. 1), the machine operates with MTPV, i.e. constant voltage ellipsis are tangent to constant torque hyperbolas. d- and q-axis in this region can be obtained by replacing the q-axis in (12) into the torque equation (4), (13) being obtained. Making the derivative of the torque with respect to the d-axis current equal to zero (3.14), produces the currents (14).

$$T_e = \frac{3}{2} P \frac{L_m^2}{L_r} i_{ds}^e \sqrt{\frac{\left(L_s i_{dqs_{rated}}\right)^2 - \left(\frac{v_{dqs_{limit}}}{\omega_e}\right)^2}{L_s^2\left(1-\sigma^2\right)}} \tag{13}$$

$$i_{ds} = \frac{v_{dqs_{limit}}}{\sqrt{2}\omega_e L_s};\ i_{qs} = \frac{v_{dqs_{limit}}}{\sqrt{2}\omega_e \sigma L_s} \tag{14}$$

C. Control strategies of IMs

High power electric drives must be able to properly operate from zero to relatively high rotational frequencies while switching frequencies are often limited to several hundred Hz. Control of the electric drive at low rotational frequencies where switching to fundamental frequency ratio is relatively large and the inverter operates far from its voltage limit, is significantly easier compared to the case of operation at high speeds characterized by reduced switching to fundamental frequency ratio and reduced (or even no) voltage margin in the inverter. Due to this, both control and modulation strategies are often dynamically changed depending on the frequency of operation [20]. A common practice in high-speed drives is using rotor flux field-oriented control (RFOC) in the low-speed range and switch to scalar or direct torque control in the high-speed range. That strategy ensures a high dynamic response of the electric drive without deterioration of the control system [21], [22].

III. Proposed remagnetization strategies for induction machines

In high-speed traction applications, the electric drive can work for certain periods of time with light loads. It is possible in this case to decrease the flux level to reduce the stator current and consequently joule losses. However, if higher torque is demanded, the machine must be magnetized first to achieve a proper flux level corresponding to the demanded torque. MTPA strategy is one of the most efficient and used strategies in motor drives for a wide speed range [23], [24]. In this paper, the map-based approach introduced in [25] will be used for selecting the current references to achieve MTPA control, taking into consideration the machine saturation. However, the main limitation of the presented map-based MTPA strategy is that it controls only the steady-state behavior of the stator current dq-axis trajectories regardless of the dynamic behavior during torque variations.

Operation with reduced flux levels will deteriorate the dynamic response of the electric drive to torque demands. The machine must be remagnetized first, where the remagnetization time is determined by the rotor time constant and by the applied magnetizing current. Generally, the goal of a remagnetization strategy is to determine the optimal torque and flux trajectories between initial ($T_{e_{ini}}$, $\lambda_{r_{ini}}$) and maximum possible torque/flux values ($T_{e_{max}}$, $\lambda_{r_{max}}$) for the corresponding speed. Due to the relatively large values of the rotor time constant fast torque changes of torque are not feasible specifically for traction applications. Fast torque variations might stress the mechanical transmission, produce wheel slip and also raise comfort concerns. Therefore, the optimization of the torque/flux trajectories should satisfy the following criteria:

- Minimization of the settling time Δt.
- Avoidance of torque impacts, i.e. sudden changes in the torque.
- Loss minimization during the transient.

in addition, other considerations must be also taken:

- Over-currents are not allowed.
- It is assumed that the load has a very large mechanical inertia, and consequently the rotor speed can be assumed to remain constant during the transient.

Some of these targets can conflict, e.g. minimization of losses and of settling time. Thus, the optimal remagnetization process may differ for each application.

Strategies for the simultaneous increase of torque and rotor flux (remagnetization) are discussed following:

A. ***Remagnetization with step-like rated d-axis change and ramp-like q-axis current change:***

If FOC is being used, the straightest remagnetization strategy to achieve rated rotor flux and torque (for the actual operating speed) is to apply the rated d- axis current as fast as possible (step increase segment 1-2 in Fig. 2a) and increase the q-axis current gradually (segment 2-3 in Fig. 2a). The main drawback of this solution is the large settling time for the torque during the machine remagnetizing process (in the range of three rotor time constants).

B. ***Remagnetization with maximum d-axis current:***

This strategy prioritizes remagnetization over torque production. As shown in Fig. 2b, following an increased torque command, all the available current is used in the d-axis for this purpose (segment 1-2 in Fig. 2b). Once the rotor flux is fully established, d-axis current is reduced to the level required to maintain the rotor flux at its target level, the remaining available current being transferred to the q-axis to produce the maximum torque (segment 2-3 in Fig. 2b). This strategy reduces the time required to produce the desired final torque (i.e. settling time) and provides the fastest torque production. However, in traction applications, fast torque variation is not allowed as mentioned above.

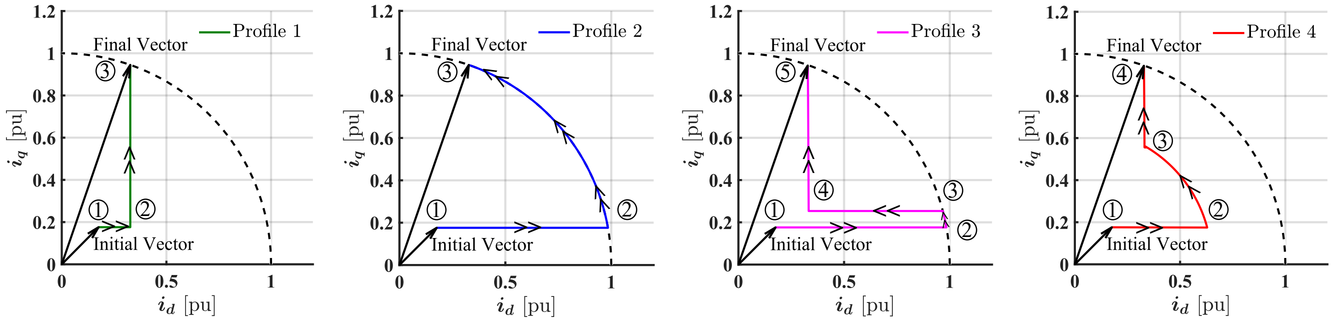

(a) (b) (c) (d)

Fig. 2: Summary of different proposed remagnetization strategies: a) step-like rated d-axis change and ramp-like q-axis current change (Profile 1); b) maximum d-axis current (Profile 2); b) maximum d-axis current and constant Nm/s (Profile 3); c) reduced d-axis current and constant Nm/s (Profile 4).

C. Remagnetization with maximum d-axis current and constant Nm/s:

The main idea behind this strategy is to control the torque to follow a ramp (15), where K_{T_e} is the slope in Nm/s.

$$T_e^* = T_{e_{ini}} + K_{T_e} t \ \ \text{for} \ \ t_1 < t < t_2 \tag{15}$$

To minimize the settling time of flux, K_{T_e} must be selected such that the maximum current is used during the whole transient (16).

$$\sqrt{{i_{ds}^*}^2 + {i_{qs}^*}^2} = I_{s_{max}} \tag{16}$$

The desired torque and flux trajectories can be obtained by solving (3), (4) and (16). Analytical solution of this system is not feasible, numerical methods can be used instead. It is seen that at the beginning of the transient all the available current is transferred to the d-axis current (segment 1-2 in Fig. 2c), the remaining current being transferred to the q-axis to establish the rotor flux quickly (segment 2-3 in Fig. 2c). Then, the d-axis current is reduced to its rated value (segment 3-4 in Fig. 2c) while increasing the q-axis current smoothly taking into consideration that fast changes in q-axis current are avoided as they would produce torque impacts (segment 4-5 in Fig. 2c).

D. Remagnetization with reduced d-axis current and constant Nm/s:

The strategy in Fig. 2d provides the same torque ramp as in Fig. 2c but uses the smallest possible current during segment 2-3. This reduces the stress in the power devices, as well as the risk of surpassing the maximum current in case of overshoot due to controller detuning. Thus, the segment 3-4 in Fig. 2c is omitted to have a continuous trajectory of d-q axis currents. However, this strategy is not straightforward, and the minimum current value changes depending on the initial torque value. One of the possible solutions is to assign profile 3 strategy with a lower current magnitude but at cost of longer magnetization time.

The proposed remagnetization strategy (see Fig. 3) includes the following process:

1) At light load, the initial rotor flux reference value is obtained from MTPA method using a look-up table or polynomial function approximation according to the operating speed.
2) Once an increase/decrease is detected in the reference torque, the torque and rotor flux references will follow one of the predefined trajectories (see Fig. 2) with rates limited to the application until reach to the new target values.
3) The rotor flux reference is limited in the field-weakening region according to the operating speed.
4) The rotor flux trajectory can be a ramp, exponential convergence or other profiles obtained from optimization methods (profiles 1-to-4, in this paper) that meets the application constraints.

The aforementioned remagnetization profiles will be simulated and evaluated in section IV.

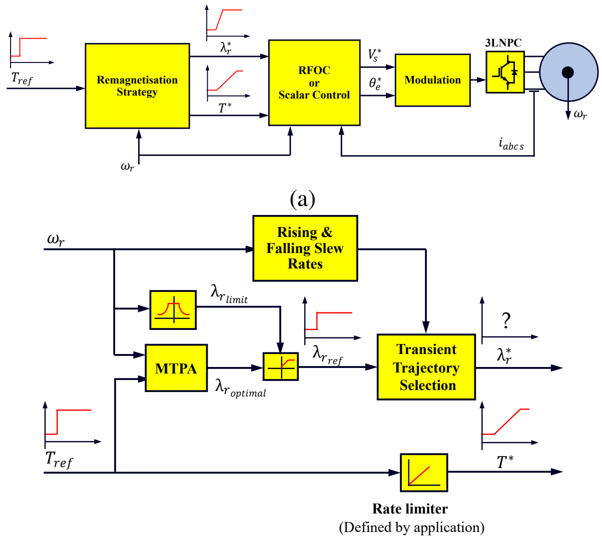

(a)

(b)

Fig. 3: Proposed remagnetization strategy: a) overall control scheme; b) detailed block diagram of the proposed method.

IV. Simulation results and experimental validation

The proposed remagnetization strategies discussed in section III have been simulated using MATLAB environment with a sample time of 200 μs. The dynamic d-q model in rotor flux reference frame is used for modeling the induction machine. IM parameters for the base speed are given in Table I.

TABLE I: Specifications of the IM at base speed (107 Hz).

Parameter	Value	Unit
DC-link voltage, (V_{dc})	3600	V
Rated Power	1084	kW
Rated Voltage, (V_{LL}, RMS)	2727	V
Pole-pairs (P)	2	-
Stator resistance (R_s)	55.38	mΩ
Stator inductance (L_s)	26.45	mH
Torque	3241	Nm
Speed	3194	rpm

Fig. 4 shows a summary of the simulation results for the machine operating at base speed, assuming that the IM is connected to an ideal inverter (i.e. linear voltage source). The IM torque is increased from 10% to 100% of the rated torque at t=0.25 s following the four remagnetization profiles proposed in subsections III-A, III-B, III-C and III-D respectively. It is noted that the slowest torque production is obtained by magnetizing the machine with profile 1, i.e. d-axis current is increased to its rated value then the q-axis current is increased gradually. The final torque will be achieved when the machine flux is fully established which could take some time (≈ 3 to 4 times the rotor time constant see Fig. 4).

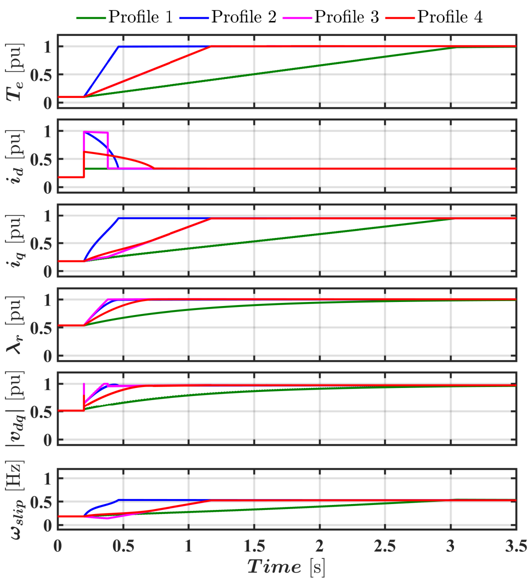

Fig. 4: Simulation results: Time response of different proposed remagnetization strategies.

On the other side, the fastest torque production is reached

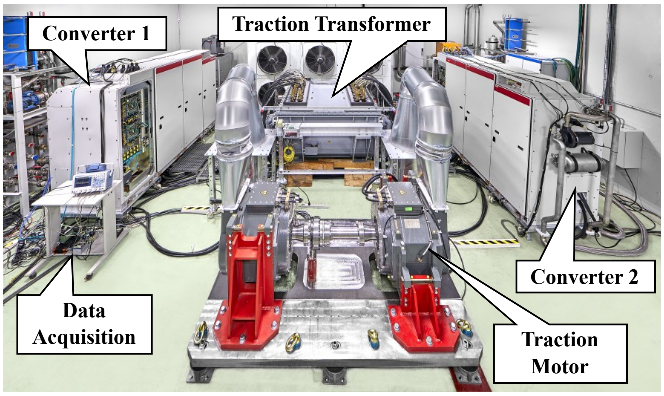

Fig. 5: Overall view of the full scale high-power traction test bench.

following profile 2 (see the blue color in Fig. 4) where all the stator current is used to magnetize the machine. Afterward, the stator current vector follows the current limit trajectory sharing the remaining current into the q-axis component assuring that the total current is not surpassed.

Profiles 3 and 4 show similar torque production rates (magenta vs. red color in Fig. 4) as these strategies are designed to follow a predefined kNm/s rate (in this application 3 kNm/s is used), however, each strategy dynamically behaves different. Profile 3 prioritize the use of stator current vector on the d-axis component in order to expedite flux establishment then the priority moves to the q-axis component for torque production (see second sub-figure Fig. 4). A reduced remaganetization can be used for profile 4 which will penalize the dynamic response of the rotor flux which is not a concern in traction applications as a fast torque increase is not needed. The main advantage of this strategy is it balances the dynamic response of the remaganetization process with the current stress on the switches of the inverter.

The proposed remagnetization strategy has been experimentally validated using high-power traction system test bench shown in Fig. 5. It consists of two identical IMs and two converters connected back-to-back, which are supplied from a High-Voltage (HV) dc power supply. The power converter module consists of a three-phase, three-level Neutral-Point Clamped (NPC) inverter feeding the IMs. Single-phase inverters feed auxiliary loads, such as cooling systems, control power supply units, etc. A dc-dc chopper is implemented for dissipative braking and dc bus overvoltage protection. A specially designed traction transformer is used to filter off catenary harmonics and allow the interconnection of the different converters. A 100 Hz (2f) filter is included in the dc bus. Preliminary experimental results for a full-scale high-speed traction drive are presented in the following. The control uses RFOC at low speeds and closed-loop scalar control at high speeds. The main system parameters are the same as those used in the simulation shown in table I.

The proposed remagnetization strategy is validated by comparing the conventional magnetization solution (applying maximum possible flux for the full speed range see Fig. 6a) against the proposed remagnetization profile 4 (see Fig. 6b). It is noted that both methods are able to reach the target torque with the same increase rate (3 kNm/s) from 10% to 100% of the rated torque. The main difference can be seen in the rotor flux for the proposed method where it is reduced to $\approx$ 48% of the rated value during light load operation compared to the conventional solution. The corresponding d- and q-axis currents are shown in the bottom figures of Fig. 6. The d-axis current is kept at its rated value for the conventional magnetization method while the d-axis current is initially reduced during light load duration then it superpassed its rated value to build up the rotor flux quickly when the torque increase is commanded. Once the machine is fully magnetized, the d-axis current is decreased to prioritize the usage of q-axis current.

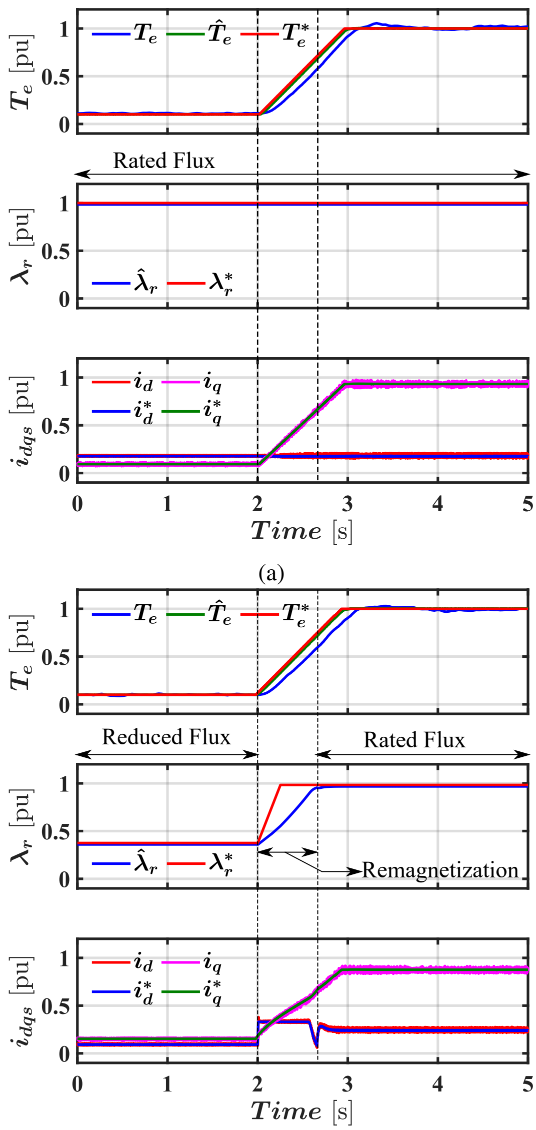

(a)

(b)

Fig. 6: Experimental results of IM torque increase from 10% to 100% of rated torque: a) applying rated magnetizing current; b) proposed remagnetization strategy.

V. Conclusions

Optimal efficiency and loss minimization control techniques have been proposed in the technical literature for optimally distributing stator current components (i.e. flux and torque producing components) while the electric machine is operating at light loads. MTPA method is commonly used in electric drives providing maximum available torque with minimum losses. However, MTPA algorithms provide the steady-state set points for the electric drive control, transients being uncontrolled and dictated by the machine time constant and the coupling between torque and flux components. Few approaches attempting to improve the torque transient response can be found in the literature. Computational complexity and approximated solutions for specific conditions limit the widespread usage of those approaches in the industry.

This paper proposes different remagnetization strategies for induction machines during torque transients. Based on the application, the remagnetization strategy can be selected to prioritize the torque dynamic response where the machine can operate at inverter limits for a portion of time. Another solution is to operate far from inverter limits at the cost of a lower dynamic response. Compromising dynamic response with system operational requirements would be the optimum solution.

The proposed remagnetization strategy calculates the initial rotor flux using MTPA algorithm at light loads. Once a change in torque command is detected, the torque and rotor flux reference will follow predefined trajectories till reach the final value. The proposed strategy at four different torque and flux components trajectories is evaluated through simulations. For traction applications, a fast dynamic response is not required as the torque rate change is limited to avoid torque shocks. Thus, a reduced remagnetizing current with constant torque increase rate has been validated experimentally through a full-scale high-power traction test bench. Currently, the proposed remagnetization torque and flux trajectories are implemented offline and stored in look-up tables. Online implementation of the remagnetization trajectory is ongoing.

References

[1] ENERGY EFFICIENCY & RENEWABLE ENERGY Office, "U.S. DRIVE electrical and electronics technical team roadmap", 2017 [Online] Available: https://www.energy.gov/eere/vehicles/downloads/us-drive-electrical-and-electronics-technical-team-roadmap.

[2] C. Liu, "Emerging electric machines and drives—an overview," *IEEE Transactions on Energy Conversion*, vol. 33, no. 4, pp. 2270–2280, 2018.

[3] Z. Yang, F. Shang, I. P. Brown, and M. Krishnamurthy, "Comparative study of interior permanent magnet, induction, and switched reluctance motor drives for EV and HEV applications," *IEEE Transactions on Transportation Electrification*, vol. 1, no. 3, pp. 245–254, 2015.

[4] J.-R. Riba, C. López-Torres, L. Romeral, and A. Garcia, "Rare-earth-free propulsion motors for electric vehicles: A technology review," *Renewable and Sustainable Energy Reviews*, vol. 57, pp. 367–379, 2016.

[5] V. T. Buyukdegirmenci, A. M. Bazzi, and P. T. Krein, "Evaluation of induction and permanent-magnet synchronous machines using drive-cycle energy and loss minimization in traction applications," *IEEE Transactions on Industry Applications*, vol. 50, no. 1, pp. 395–403, 2013.

[6] L. Buhrkall, “Traction system case study,” in *The 9th Institution of Engineering and Technology Professional Development Course on Electric Traction Systems*. IET, 2006, pp. 53–71.

[7] G. Pellegrino, A. Vagati, B. Boazzo, and P. Guglielmi, “Comparison of induction and PM synchronous motor drives for EV application including design examples,” *IEEE Transactions on industry applications*, vol. 48, no. 6, pp. 2322–2332, 2012.

[8] D. S. Kirschen, D. W. Novotny, and W. Suwanwisoot, “Minimizing induction motor losses by excitation control in variable frequency drives,” *IEEE Transactions on Industry Applications*, no. 5, pp. 1244–1250, 1984.

[9] D. Biswas, K. Mukherjee, and N. C. Kar, “A novel approach towards electrical loss minimization in vector controlled induction machine drive for EV/HEV,” in *2012 IEEE Transportation Electrification Conference and Expo (ITEC)*. IEEE, 2012, pp. 1–5.

[10] R. Tarvirdilu-Asl, S. Nalakath, Z. Xia, Y. Sun, J. Wiseman, and A. Emadi, “Improved online optimization-based optimal tracking control method for induction motor drives,” *IEEE Transactions on Power Electronics*, vol. 35, no. 10, pp. 10 654–10 672, 2020.

[11] D. S. Kirschen, D. W. Novotny, and T. A. Lipo, “On-line efficiency optimization of a variable frequency induction motor drive,” *IEEE transactions on industry applications*, no. 3, pp. 610–616, 1985.

[12] S. Bozhko, S. Dymko, S. Kovbasa, and S. M. Peresada, “Maximum torque-per-amp control for traction im drives: Theory and experimental results,” *IEEE Transactions on Industry Applications*, vol. 53, no. 1, pp. 181–193, 2016.

[13] S. N. Vukosavic and E. Levi, “A method for transient torque response improvement in optimum efficiency induction motor drives,” *IEEE transactions on energy conversion*, vol. 18, no. 4, pp. 484–493, 2003.

[14] J.-F. Stumper, A. Dötlinger, and R. Kennel, “Loss minimization of induction machines in dynamic operation,” *IEEE transactions on energy conversion*, vol. 28, no. 3, pp. 726–735, 2013.

[15] Z. Hu, Q. Liu, and K. Hameyer, “Loss minimization of speed controlled induction machines in transient states considering system constraints,” in *2014 17th International Conference on Electrical Machines and Systems (ICEMS)*. IEEE, 2014, pp. 123–129.

[16] A. Popov, V. Lapshina, I. Gulyaev, and F. Briz, “Improving the dynamic response of FOC induction machines operated with reduced rotor flux,” in *2018 25th International Workshop on Electric Drives: Optimization in Control of Electric Drives (IWED)*. IEEE, 2018, pp. 1–4.

[17] P. C. Krause and C. Thomas, “Simulation of symmetrical induction machinery,” *IEEE transactions on power apparatus and systems*, vol. 84, no. 11, pp. 1038–1053, 1965.

[18] A. M. Khambadkone and J. Holtz, “Vector-controlled induction motor drive with a self-commissioning scheme,” *IEEE Transactions on Industrial Electronics*, vol. 38, no. 5, pp. 322–327, 1991.

[19] F. Blaschke, “The principle of field orientation as applied to the new transvektor closed-loop control system for rotating field machines,” *Siemens review*, vol. 34, no. 1, 1972.

[20] A. Fathy Abouzeid, J. M. Guerrero, A. Endemaño, I. Muniategui, D. Ortega, I. Larrazabal, and F. Briz, “Control strategies for induction motors in railway traction applications,” *Energies*, vol. 13, no. 3, p. 700, 2020.

[21] T. H. Nguyen, T. L. Van, D.-C. Lee, J.-H. Park, and J.-H. Hwang, “Control mode switching of induction machine drives between vector control and v/f control in overmodulation range,” *Journal of Power Electronics*, vol. 11, no. 6, pp. 846–855, 2011.

[22] A. F. Abouzeid, J. M. Guerrero, I. Muniategui, A. Endemaño, D. Ortega, and F. Briz, “Torque dynamics enhancement of railway traction drives using scalar control,” in *2021 IEEE International Electric Machines & Drives Conference (IEMDC)*. IEEE, 2021, pp. 1–6.

[23] O. Wasynczuk, S. Sudhoff, K. Corzine, J. L. Tichenor, P. Krause, I. Hansen, and L. Taylor, “A maximum torque per ampere control strategy for induction motor drives,” *IEEE Transactions on Energy Conversion*, vol. 13, no. 2, pp. 163–169, 1998.

[24] H. Kouns, J.-S. Lai, and C. E. Konrad, “Analysis of a traction induction motor drive operating under maximum efficiency and maximum torque per ampere conditions,” in *Nineteenth Annual IEEE Applied Power Electronics Conference and Exposition, 2004. APEC'04.*, vol. 1. IEEE, 2004, pp. 545–551.

[25] R. Bojoi, Z. Li, S. Odhano, G. Griva, and A. Tenconi, “Unified direct-flux vector control of induction motor drives with maximum torque per ampere operation,” in *2013 IEEE Energy Conversion Congress and Exposition*. IEEE, 2013, pp. 3888–3895.

VI. BIOGRAPHIES

Ahmed Fathy Abouzeid (M'19) received the B.S and M.S. degrees in Electrical Engineering from Port Said University, Port Said, Egypt, in 2012 and 2017, respectively. He is currently pursuing his Ph.D. Degree at the Department of Electrical, Electronic and Computer Engineering, University of Oviedo, Gijón, Spain. In 2013, he joined the Department of Electrical Engineering, Port Said University, Egypt, as a Teaching Assistant. Currently, he is on leave with the same department as an Assistant Lecturer. He is partially supported by a scholarship from the Ministry of Higher Education and Scientific Research of Egypt. His research interests include power converters and ac drives, electric traction, and renewable energy systems.

Juan M. Guerrero (S'00–A'01–M'04–SM'21) received the M.E. degree in industrial engineering and the Ph.D. Degree in Electrical and Electronic Engineering from the University of Oviedo, Gijón, Spain, in 1998 and 2003, respectively. Since 1999, he has occupied different teaching and research positions with the Department of Electrical, Computer and Systems Engineering, University of Oviedo, where he is currently an Associate Professor. From February to October 2002, he was a Visiting Scholar at the University of Wisconsin, Madison. From June to December 2007, he was a Visiting Professor at the Tennessee Technological University, Cookeville. He is Associate Editor of the IEEE Trans. on Industry Applications. His research interests include control of electric drives and power converters, electric traction, and renewable energy generation.

Iban Vicente-Makazaga graduated in electrical engineering from University of Mondragon, Mondragon, Spain, in 2003 and the M.S. and the Ph.D. degrees from the University of Manchester, UK, in 2004 and 2009 respectively. He joined Ingeteam Power Technology (formerly TEAM), Zamudio, Spain, where he works as a Control and Regulation Engineer involved in railway traction control for trams, locomotives and EMU-s. His current research interests include power converter and advanced control drives, modulation techniques, machine parameters and speed estimation techniques as well railway research issues such as AC catenary stability and mechanical vibrations in the drive-train.

Iker Muniategui-Aspiazu received the Industrial Technical Engineering Degree (Electronic Design speciality) and the Industrial Automatics and Electronics Engineering Degree, from the University of Mondragon, Mondragon, Spain, in 2004 and 2007 respectively. In September 2006, he joined Ingeteam Power Technology (formerly TEAM), Zamudio, Spain, where he worked as a Control and Regulation Engineer, and he is currently Control and Regulation manager of Traction department. His current research interests include power converter and advanced control drives, modulation techniques, railway research issues such as AC catenary stability and mechanical vibrations in the drive-train.

Aitor Endemaño-Isasi received the Industrial Technical Engineering Degree (Electronic Design speciality) and the Industrial Automatics and Electronics Engineering Degree, from the University of Mondragon, Mondragon, Spain, in 1997 and 2000 respectively, and the PhD from Heriot-Watt University, Edinburgh, Scotland, UK, in 2003. In 2003 he joined Traction department at Ingeteam Power Technology (formerly TEAM), Zamudio, Spain, where since then he has been a Control and Regulation Engineer, involved in several traction control design projects for trams, locomotives and EMU-s. His current research interests include power converter and advanced control drives, modulation techniques, railway research issues such as AC catenary stability and mechanical vibrations in the drive-train.

Fernando Briz (A'96–M'99–SM'06) received the M.S. and Ph.D. degrees from the University of Oviedo, Gijón, Spain, in 1990 and 1996, respectively. He is currently a Full Professor with the Department of Electrical, Computer and Systems Engineering, University of Oviedo. Dr. Briz received an IEEE TRANSACTIONS ON INDUSTRY APPLICATIONS Award and nine IEEE Industry Applications Society Conference and IEEE Energy Conversion Congress and Exposition prize paper awards. He is Past Chair of the Industrial Drives Committee of the Industrial Power Conversion System Department (IPCSD) of the IAS. Currently he is Vice Chair of IPCSD. He has served in scientific committees and as Vice Chair or Technical Program Chair of several conferences, including ECCE, IEMDC, ICEM, ICEMS and SLED. He is a Member of the Steering Committee of IEEE Journal of Emerging and Selected Topics in Power Electronics (JESTPE), Editor of JESTPE Transactions and Associate Editor of IAS Transactions. His topics of interest include electronic power converters and ac drives, power systems, machine monitoring and diagnostics and digital signal processing.